

# Elementary $[Ca^{2+}]_i$ signals generated by electroporation functionally mimic those evoked by hormonal stimulation

FEDJA BOBANOVIC,<sup>\*,†</sup> MARTIN D. BOOTMAN,<sup>\*,†,1</sup> MICHAEL J. BERRIDGE,<sup>\*,‡</sup>  
NICOLA A. PARKINSON,<sup>\*,2</sup> AND PETER LIPP\*

\*Laboratory of Molecular Signalling, Babraham Institute, Cambridge, England, U.K.; <sup>†</sup>Laboratory of Biocybernetics, Faculty of Electrical Engineering, University of Ljubljana, Slovenia; and <sup>‡</sup>Department of Zoology, University of Cambridge, Cambridge, England, U.K.

**ABSTRACT** The generation of oscillations and global  $Ca^{2+}$  waves relies on the spatio-temporal recruitment of elementary  $Ca^{2+}$  signals, such as 'Ca<sup>2+</sup> puffs'. Each elementary signal contributes a small amount of  $Ca^{2+}$  into the cytoplasm, progressively promoting neighboring  $Ca^{2+}$  release sites into an excitable state. Previous studies have indicated that increases in frequency or amplitude of such hormone-evoked elementary  $Ca^{2+}$  signals are necessary to initiate  $Ca^{2+}$  wave propagation. In the present study, an electroporation device was used to rapidly and reversibly permeabilize the plasma membrane of HeLa cells and to allow a limited influx of  $Ca^{2+}$ . With low field intensities (100–500 V/cm), brief (50–100  $\mu$ s) electroporation triggered localized  $Ca^{2+}$  signals that resembled hormone-evoked  $Ca^{2+}$  puffs, but not global signals. With such low intensity electroporative pulses, the  $Ca^{2+}$  influx component was usually undetectable, confirming that the electroporation-induced local signals represented  $Ca^{2+}$  puffs arising from the opening of intracellular  $Ca^{2+}$  release channels. Increasing either the frequency at which low-intensity electroporative pulses were applied, or the intensity of a single electroporative pulse (>500 V/cm), resulted in caffeine-sensitive regenerative  $Ca^{2+}$  waves. We suggest that  $Ca^{2+}$  puffs caused by electroporation functionally mimic hormone-evoked elementary events and can activate global  $Ca^{2+}$  signals if they provide a sufficient trigger.—Bobanović, F., Bootman, M. D., Berridge, M. J., Parkinson, N. A., Lipp, P. Elementary  $[Ca^{2+}]_i$  signals generated by electroporation functionally mimic those evoked by hormonal stimulation. *FASEB J.* 13, 365–376 (1999)

*Key Words:*  $Ca^{2+}$  puffs •  $Ca^{2+}$  waves • HeLa cells • confocal microscopy •  $InsP_3$  receptors

HORMONAL STIMULATION of many cell types triggers production of the  $Ca^{2+}$ -mobilizing messenger inositol 1,4,5-trisphosphate ( $InsP_3$ ),<sup>3</sup> which activates repetitive intracellular  $Ca^{2+}$  ( $[Ca^{2+}]_i$ ) oscillations (1, 2). The subcellular correlate of  $[Ca^{2+}]_i$  oscillations

are waves, where  $[Ca^{2+}]_i$  is initially elevated in a localized region of a cell and then propagates across the entire cell in a regenerative manner. Recent evidence has suggested that such global  $[Ca^{2+}]_i$  oscillations and waves are generated by the recruitment of elementary  $Ca^{2+}$  release events, such as 'Ca<sup>2+</sup> puffs' (3, 4), and 'Ca<sup>2+</sup> sparks' (5–7; for reviews, see refs 8–11).

We previously observed that  $Ca^{2+}$  puffs both initiated and propagated  $Ca^{2+}$  waves in hormonally stimulated HeLa cells (4). The  $Ca^{2+}$  puffs evoked during agonist stimulation of HeLa cells are highly localized  $Ca^{2+}$  signals (~6  $\mu$ M in diameter), arising from clusters of  $InsP_3$  receptors ( $InsP_3Rs$ ) spaced ~6  $\mu$ m apart (4). They occur stochastically during cell stimulation, and unless adjacent elementary  $Ca^{2+}$  release sites become functionally coupled their  $Ca^{2+}$  signals remain spatially confined (12). Essentially, each  $Ca^{2+}$  puff contributes a small quantum (a few attomoles) of  $Ca^{2+}$  into the cytoplasm. When the  $Ca^{2+}$  puff sites operate at low frequencies or amplitudes, the released  $Ca^{2+}$  can be effectively buffered or resequenced by the cell. However, with sufficient activity, the released  $Ca^{2+}$  can overwhelm the cellular buffering mechanisms, leading to a progressive  $[Ca^{2+}]_i$  increase that eventually triggers a regenerative  $Ca^{2+}$  wave (12, 13).

In the present study, we used an electroporation device to evoke spatially restricted, rapid and reversible influx of  $Ca^{2+}$  into HeLa cells. Electroporation essentially involves the application of a high-intensity electric field across a cell, leading to changes in plasma membrane potential that cause a localized breakdown of the lipid bilayer (14–16). The electro-

<sup>1</sup> Correspondence: Laboratory of Molecular Signalling, Babraham Institute, Babraham, CB2 4AT, Cambridge, U.K. E-mail: martin.bootman@bbsrc.ac.uk

<sup>2</sup> Present address: Department of Physiology, University College London, Gower Street, London, WC1E 6BT.

<sup>3</sup> Abbreviations:  $[Ca^{2+}]_i$ , intracellular  $Ca^{2+}$ ; EM, external medium;  $InsP_3$ , inositol 1,4,5-trisphosphate;  $InsP_3R$ ,  $InsP_3$  receptor; PLC, phospholipase C; RyR, ryanodine receptor.

poration effect is a localized phenomenon because not all parts of the membrane exposed to an electrical field are subject to the same change in membrane potential (17–20). In fact, the change in membrane potential, and consequently the electroporative effect, is most prominent at the restricted parts of the cell facing the electrodes (21–23), particularly the membrane facing the anode, where the membrane potential becomes hyperpolarized. The extent and duration of permeabilization can be modulated by changing parameters such as strength, duration, and repetition frequency of the electric field. The use of electroporation to evoke spatially discrete  $[Ca^{2+}]_i$  changes allowed us to test the hypothesis that the transition from local to global  $[Ca^{2+}]_i$  signals is dependent on the amplitude and frequency of elementary  $Ca^{2+}$  signals (13).

Electroporation of HeLa cells using low field intensities evoked  $Ca^{2+}$  puffs with the same spatio-temporal characteristics as hormone-evoked elementary events. These electroporation-induced signals were a consequence of the minute influx of  $Ca^{2+}$  that occurred during the rapid and transient plasma membrane disruption. Electroporation could functionally mimic the effect of a hormone on the cells in that it could trigger localized  $Ca^{2+}$  puffs or globally propagating regenerative  $Ca^{2+}$  waves.

## MATERIALS AND METHODS

### Cell culture and fura-2 measurement

HeLa cells were cultured and prepared for imaging as described previously (24). For all experiments, cells were bathed in an external medium (EM) containing (in mM: NaCl 127, KCl 5,  $MgCl_2$  2,  $NaH_2PO_4$  0.5,  $NaHCO_3$  5, HEPES 10, glucose 10,  $CaCl_2$  1.8; pH 7.4). All experiments were carried out at room temperature (20–22°C).

For video imaging studies, a coverslip of fura-2-loaded cells was mounted in a homemade electroporabilization chamber (see below). The chamber was placed on the stage of a Nikon Diaphot 300 inverted microscope. Video images were obtained using an intensified CCD camera (COHU, San Diego, Calif.), stepping filter wheel (Rainbow; Life Sciences Resources Ltd., U.K.), and Merlin acquisition system (Life Science Resources Ltd., Cambridge, U.K.). The cells were alternately excited at 340 nm and 380 nm using a 75W Xenon lamp in conjunction with 7.5 HBW filters (Omega Optical, Dallas, Tex.); fluorescence emission was measured at 510 nm (1 image per second).  $[Ca^{2+}]_i$  was estimated from the 340 nm/380 nm fluorescence ratio according to the equation:  $[Ca^{2+}]_i = K_d \times \beta ((R-R_{min})/(R_{max}-R))$  (25).  $R_{min}$  and  $R_{max}$  were determined empirically by permeabilizing the cells to  $Ca^{2+}$  using 5  $\mu$ M ionomycin (Sigma, Poole, Dorset, U.K.) and exposing the cells to extracellular solutions of high (10 mM) and low  $Ca^{2+}$  (no added  $CaCl_2$  +10 mM EGTA). Typical values obtained were  $R_{min} = 0.15$ ,  $R_{max} = 2$ . The dissociation constant,  $K_d$ , was taken to be 225 nM (25). Experiments investigating  $Mn^{2+}$  quench of fura-2 were performed using standard EM supplemented with 250  $\mu$ M  $MnCl_2$ . The fluorescent indicator was excited in  $Ca^{2+}$ -insensitive absorption wavelength 360 nm (isosbestic point).

### Confocal imaging

Confocal images were obtained using a Noran Oz laser-scanning confocal microscope (Noran, Milton Keynes, U.K.). Fluo-3-loaded cells mounted in the electroporation chamber were placed on the stage of a Nikon Diaphot 300 microscope. Fluo-3 was excited using the 488 nm line of an argon-ion laser, and the fluorescence emission was collected at wavelengths  $>505$  nm. The confocal slit was chosen to give a 'z' resolution of  $\sim 1$   $\mu$ m. Images were acquired with a rate of 7.5 images per second. Data processing was performed as described previously (4).

Measurements of relative membrane potential changes were performed using di-8-ANEPPS-loaded cells as described by Hüser et al. (26). The cells were loaded with di-8-ANEPPS by incubation with a 5  $\mu$ M concentration of the dye for 10 min. Di-8-ANEPPS was excited at 514 nm and the fluorescence emission was monitored at wavelengths of  $>525$  nm. To follow the rapid membrane potential changes with sufficient temporal resolution, we used the line-scan mode of the confocal microscope (250 ns/line).

### Electroporation

Electroporation was performed using a homemade system capable of generating mono- and bipolar square electrical pulses, with amplitudes ranging from 0 to 2000 V and a duration of 1 to 1000  $\mu$ s. The amplitude and the waveform of the electric field exposure were monitored using a digital storage oscilloscope (Tektronix, Beaverton, Oreg.). The electroporation system essentially consists of a Perspex chamber with two electrodes connected to a high-frequency voltage source. The volume of the rectangular chamber (50  $\mu$ l) was kept as small as possible to enable the application of a uniform electric field simultaneously with a consistent rapid perfusion of EM. The cells used for the experiments were located in the central part of the narrow (3 mm) chamber filled with EM that brings into contact two platinum electrodes. Perfusion of cells in the electroporation chamber avoids artifacts resulting from the generation of electrolysis by-products, such as  $O_2$  and  $H_2$ . The temperature of the extracellular solution was unaffected by the electrical pulse (data not shown).

For video imaging studies, square monopolar pulses of either 10 or 50  $\mu$ s duration were used. For the confocal studies, a square bipolar pulse of 50  $\mu$ s duration in both directions (100  $\mu$ s total duration) was applied in order to increase the chances of finding responsive cells at near-threshold levels of stimulation. For the confocal studies using di-8-ANEPPS, where changes in membrane potential were monitored, longer pulses of 1 ms were used.

## RESULTS

### Electroporation-induced $[Ca^{2+}]_i$ signals

Initial experiments characterized the source and nature of the electroporation-induced  $[Ca^{2+}]_i$  signals in HeLa cells. Electroporation of cells reproducibly evoked  $Ca^{2+}_i$  increases in the presence of extracellular  $Ca^{2+}$  ( $Ca^{2+}_o$ ) (Fig. 1A). After removal of  $Ca^{2+}_o$  such responses were absent, which suggests they were due, or at least triggered by, a  $Ca^{2+}$  influx. In most cells the response consisted of a single

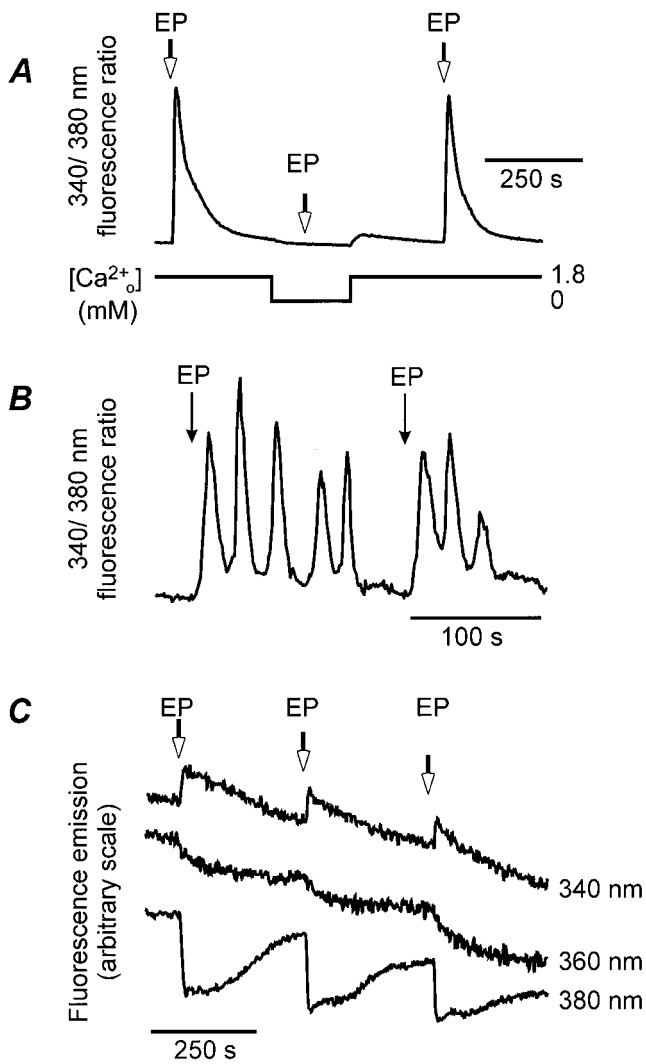


**Figure 1.** Electroporation evokes transient increases in  $Ca^{2+}$  resulting from inward cation flux. Panel A represents an averaged response of fura-2-loaded HeLa cells to three electroporative pulses (denoted by vertical arrows marked EP) in the presence or absence of  $Ca^{2+}_o$ . B) An oscillatory  $Ca^{2+}$  signal arising from a cell in  $Ca^{2+}$ -containing medium stimulated with a single electroporative pulse. This pattern of response was seen in a minority of cells. C) The extracellular medium was supplemented with 250  $\mu$ M  $MnCl_2$  and the fluorescence emission at 510 nm was monitored for 340, 360, and 380 nm excitation. The traces show that each  $[Ca^{2+}]_i$  rise coincided with a transient increase in the rate of cation entry. The electroporative pulses (EP) (A, C, 1000 V/cm, 50  $\mu$ s duration, monopolar; B, 700 V/cm, 10  $\mu$ s duration) were applied at the times shown by vertical arrows. The effect of field intensity on  $Mn^{2+}$  quench of fura-2 was qualitatively similar in the presence or absence of  $Ca^{2+}_o$  (data not shown), confirming that neither the absence of  $Ca^{2+}_o$  in the bathing media nor a  $[Ca^{2+}]_i$  increase affected the sensitivity of the cells to electroporation. Panel A represents an average response ( $n=37$ ); panels B and C illustrate typical responses from single cells.

transient  $[Ca^{2+}]_i$  increase, although in some cells (<10%;  $n>2000$ ) a single electroporative pulse triggered a series of progressively diminishing  $[Ca^{2+}]_i$  oscillations (Fig. 1B).

The stepwise quench of fura-2 by  $Mn^{2+}$  (Fig. 1C) confirmed that the cation permeability of the cells increased with each electroporative pulse. Over the range of 0.6–1 kV/cm, both the quench of fura-2 by  $Mn^{2+}$  and the corresponding increases in  $[Ca^{2+}]_i$  showed a supralinear relationship to the field intensity (Fig. 2A, B). These data indicate that increasing electroporative potentials cause greater cation entry and that at a field intensity of  $\sim 700$  V/cm, a threshold was reached where  $[Ca^{2+}]_i$  responses were greatly enhanced (Fig. 2A; filled squares). In cells where  $[Ca^{2+}]_i$  oscillations were initiated by a single

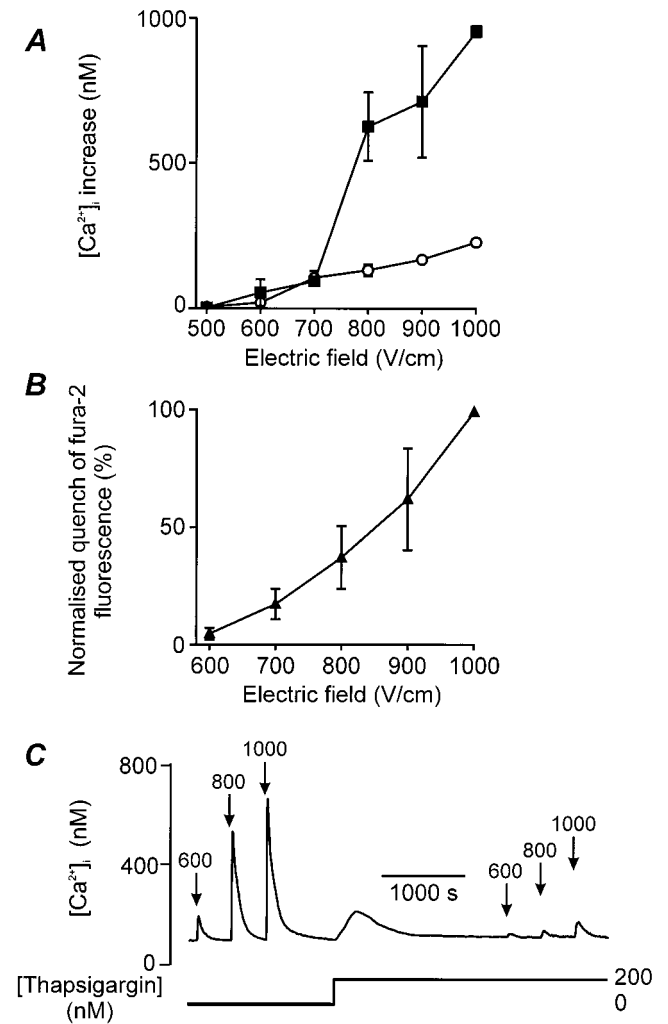


**Figure 2.** Electroporation-induced  $Ca^{2+}$  increases are determined by the magnitude of the applied field and are inhibited by caffeine and thapsigargin. A) The amplitude of  $[Ca^{2+}]_i$  increase triggered by application of different intensity electroporative fields in the absence (filled squares) or presence (open circles) of 20 mM caffeine. The extent of cation entry into the cells was also dependent on the field intensity, as illustrated in panel B. B) The data are presented as mean  $\pm$  SEM ( $n$  between 6 and 26). C) Electroporation-induced  $[Ca^{2+}]_i$  increases were reduced to  $\sim 10\%$  of the control response ( $n=38$ ) by treating the cells with thapsigargin to remove functional  $Ca^{2+}$  stores. The electroporation pulses used to obtain the data shown in this figure were monopolar and 50  $\mu$ s in duration.

electroporative pulse (e.g., Fig. 1B), the  $Mn^{2+}$  quench of fura-2 revealed a single cation entry step simultaneous with the electroporation pulse, but no further discrete steps during the subsequent oscillations (data not shown).

The supralinearity of the  $[Ca^{2+}]_i$  signals (Fig. 2A) was not simply due to increasing  $Ca^{2+}$  influx at high field intensities, because the  $[Ca^{2+}]_i$  response displayed a > sixfold increase between 700 and 800 V/cm (Fig. 2A), whereas the  $Mn^{2+}$  quench response increased by only twofold (Fig. 2B). The enhancement of  $[Ca^{2+}]_i$  increases with field intensities above 700 V/cm was most likely due to amplification by  $Ca^{2+}$  release from intracellular stores, since this effect was absent during incubation of the cells in 20 mM caffeine to inhibit  $InsP_3R$  function. Caffeine reduced the amplitude of the  $[Ca^{2+}]_i$  increases seen with larger (>700 V/cm) electroporative pulses and produced an almost linear relationship between field intensity and change in  $[Ca^{2+}]_i$  (Fig. 2A; open circles). Removal of functional intracellular  $Ca^{2+}$  stores by prolonged treatment of cells with 200 nM thapsigargin substantially decreased electroporation-induced increases in  $[Ca^{2+}]_i$  (Fig. 2C), also confirming that the major portion of the  $[Ca^{2+}]_i$  signals arose from  $Ca^{2+}$  release. Although HeLa cells express ryanodine receptors (RyRs) (27, 28), these intracellular  $Ca^{2+}$  release channels did not seem to be involved in the electroporation-evoked  $[Ca^{2+}]_i$  signals, since preincubation of cells with 10  $\mu M$  ryanodine for 30 min to block RyR opening did not alter the responses (data not shown).

As illustrated in Fig. 2A, low field intensities (500–700 V/cm) did not trigger large regenerative responses. An example of the low-amplitude, non-regenerative responses obtained with such low electroporative potentials is shown in Fig. 3A. Repetitive application (1/min) of the electroporative pulse evoked only modest ( $\sim 20$  nM) increases in  $[Ca^{2+}]_i$ , which decayed back to basal levels in a matter of a few tens of seconds. But if such pulses were applied at a twofold higher frequency, they eventually triggered a regenerative response (Fig. 3B). Similarly, low-frequency (1/min) electroporative pulses applied in the presence of a low (100 nM) histamine concentration also triggered a regenerative response (Fig. 3C). This subthreshold histamine concentration was unable to evoke increases in  $[Ca^{2+}]_i$  when applied on its own for periods of up to 45 min (data not shown).

A consistent feature of  $[Ca^{2+}]_i$  increases triggered by electroporation was that they displayed desensitization if large regenerative responses were induced, and the cells needed a period of recovery before similar responses could be elicited again. For example, although pulses of 1000 V/cm evoked consistent amplitude responses when applied at low frequency

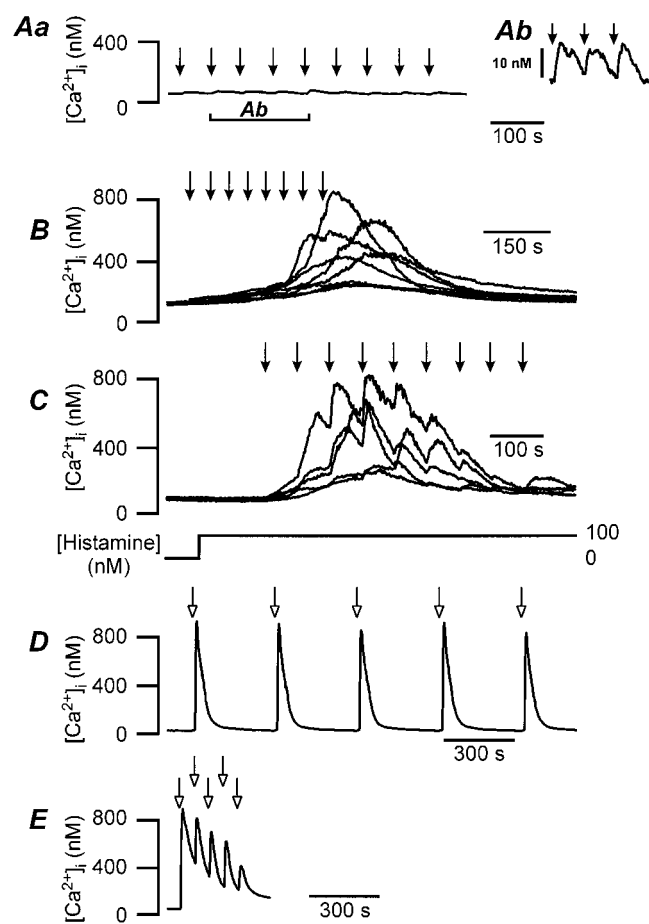


**Figure 3.** Low-frequency electroporative pulses evoke reproducible  $Ca^{2+}$  signals. Panels A–C illustrate the effect of a low-intensity electroporation (filled arrows, 700 V/cm; 10  $\mu s$  duration; monopolar) applied at 1/min (A), 1 per 30 s (B), or 1/min in the presence of a subthreshold histamine concentration (C). Panels D, E show the response to a high-intensity electroporation (open arrows, 1000 V/cm; 50  $\mu s$  duration; monopolar) applied at 1/6 min (D) or 1/min (E). A, D, E Averaged responses from 17, 23, and 21 cells, respectively. B, C) Responses from multiple individual cells. The data in Ab were obtained from the section marked in Aa, and are presented with an expanded y-axis scale.

(1/6 min, Fig. 3D), the  $[Ca^{2+}]_i$  increases triggered by the same stimulus rapidly desensitized when the frequency was increased to 1/min (Fig. 3E). Since electroporation of cells invariably caused cation entry, as measured by  $Mn^{2+}$  quenching of fura-2 (e.g., Fig. 1C), this desensitization did not reflect a progressive failure to electroporate the cells but rather the progressive failure of regenerative  $Ca^{2+}$  release.

These data suggest that electroporation caused an influx of  $Ca^{2+}$ , which subsequently evoked regenerative  $Ca^{2+}$  release from  $InsP_3R$ s on intracellular stores. This temporal sequence of events is further supported by the observations that regenerative  $[Ca^{2+}]_i$  changes could occur with a latency of tens of seconds after the electroporative pulse (see below) and that electroporation-induced  $[Ca^{2+}]_i$  oscillations could persist for several minutes (Fig. 1B).

## Electroporation triggers regenerative $[Ca^{2+}]_i$ waves, but does not stimulate $InsP_3$ production

To confirm that electroporation triggered regenerative  $Ca^{2+}$  release, we investigated the subcellular properties of the electrically stimulated  $[Ca^{2+}]_i$  transients using rapid confocal imaging. Application of suprathreshold electric fields evoked  $[Ca^{2+}]_i$  signals that began first in the regions of the cells closest to the electrodes, then propagated throughout the cells in a nondcremental manner (**Fig. 4**). Such regenerative  $[Ca^{2+}]_i$  waves could be reproducibly elicited, with the initiation points consistently being the parts of the cells most adjacent to the electrodes and with the same direction of wave propagation. The velocities of these electroporation-induced  $Ca^{2+}$  waves were only marginally less than those evoked by histamine (**Fig. 5A, C**; ref 4). Preincubation of the cells with caffeine (20 mM) markedly reduced the amplitude and velocity of such  $[Ca^{2+}]_i$  waves to more slowly diffusing signals that penetrated

through the cytoplasm in a decremental manner (**Fig. 5B, C**).

The observation that electroporation above a certain threshold led to a caffeine-inhibitable regenerative  $[Ca^{2+}]_i$  rise was surprising, since even though  $InsP_3$ Rs are sensitive to  $Ca^{2+}$ , they usually require coactivation with  $InsP_3$ . We therefore tested whether electroporation simply mimicked hormone action on HeLa cells by evoking the production of  $InsP_3$ , thereby triggering  $Ca^{2+}$  release from intracellular stores. We used the phospholipase C (PLC) inhibitor, U-73122, to prevent production of  $InsP_3$  during an electroporative pulse. U-73122 inhibited histamine-evoked  $[Ca^{2+}]_i$  signals in a concentration-dependent manner ( $IC_{50}=273$  nM; **Fig 6A**). The structural analog U-73343, which is a much less potent PLC inhibitor, did not affect histamine-evoked  $Ca^{2+}$  signals at concentrations of up to 10  $\mu$ M (**Fig. 6A**). Electroporation-induced  $[Ca^{2+}]_i$  signals were unaffected by U-73122 at concentrations that virtually abolished histamine responses (**Fig. 6C**).

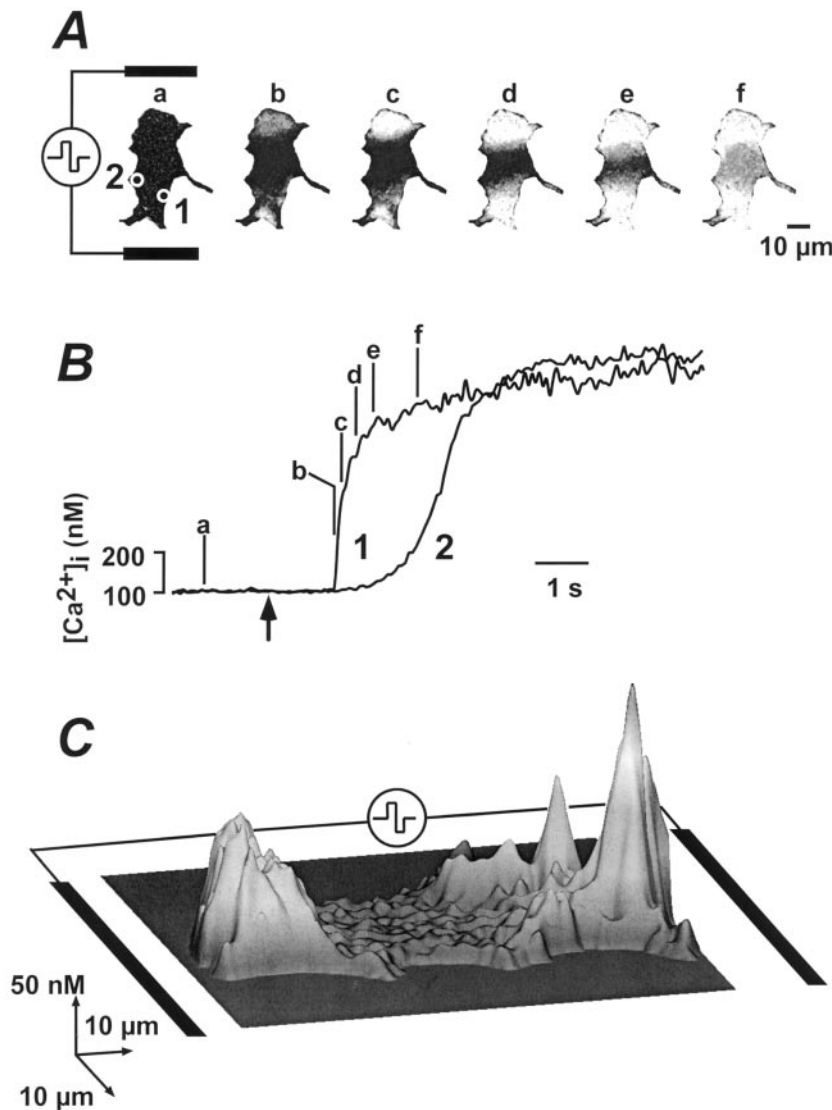


**Figure 4.** Electroporation-induced  $Ca^{2+}$  wave. Panels A, B illustrate the spatial and temporal profile of an electroporation-evoked  $Ca^{2+}$  wave in a fluo-3-loaded HeLa cell (500 V/cm; 100  $\mu$ s duration; bipolar pulse). A) A sequence of confocal images of the stimulated cell at the times indicated in panel B. The  $[Ca^{2+}]_i$  in the circular regions (1 and 2) shown in panel B are plotted in panel B. C) A surface representation of Ab demonstrating the initially inhomogeneous  $[Ca^{2+}]_i$  signal triggered by electroporation.

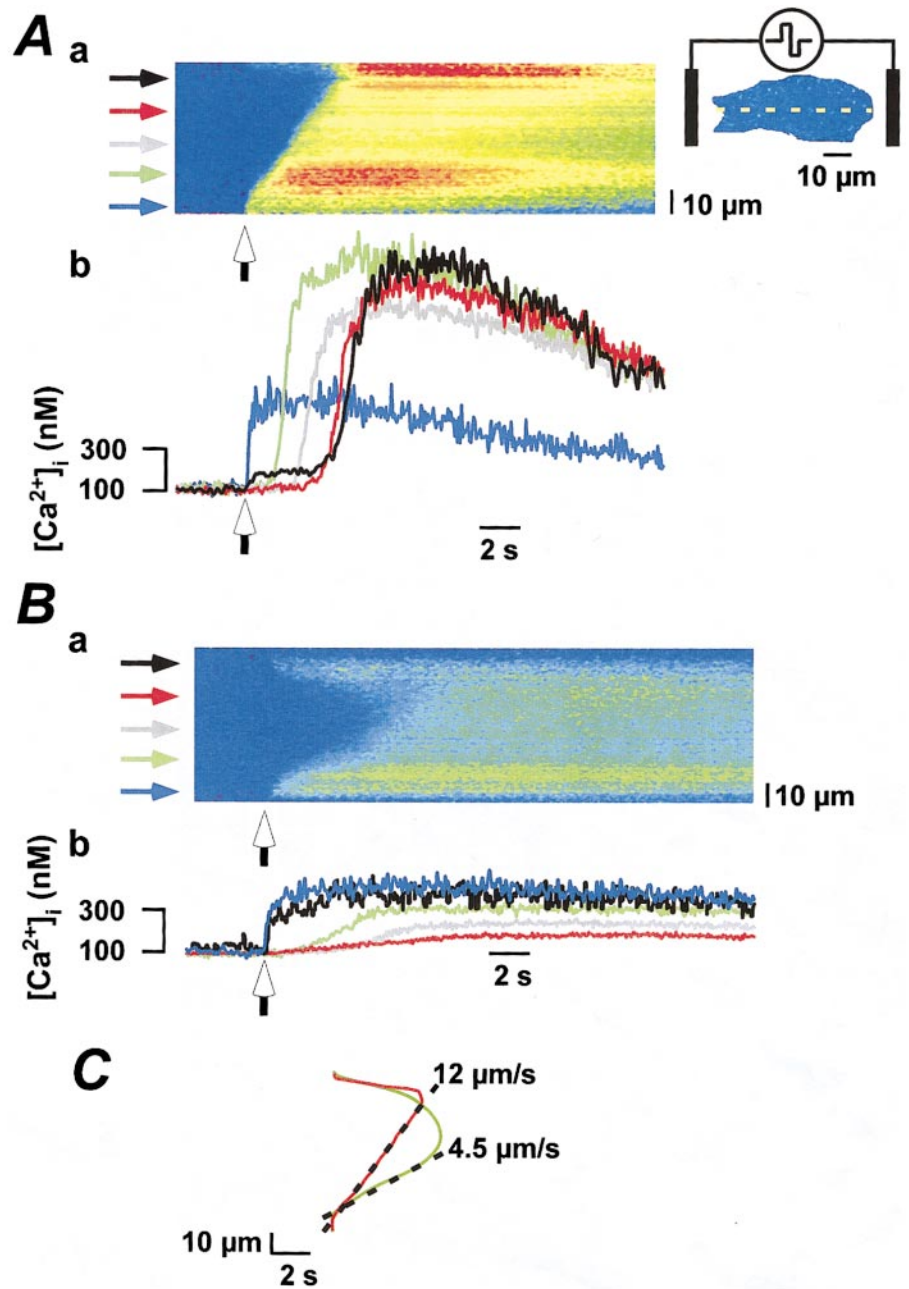


**Figure 5.** Caffeine reduces electroporation-evoked  $\text{Ca}^{2+}$  waves to a slowly diffusing low-amplitude  $[\text{Ca}^{2+}]_i$  increase. *A, B*  $[\text{Ca}^{2+}]_i$  signals triggered by repetitive electroporative pulses (500 V/cm; 100  $\mu\text{s}$  duration; bipolar pulse) applied to the same cell in the absence (*A*) or presence (*B*) of 20 mM caffeine. The electroporative pulses were applied at the vertical arrows. *Aa* and *Ba* are line-scan images of the evoked  $[\text{Ca}^{2+}]_i$  signals. *Ab* and *Bb* show the temporal profile of  $[\text{Ca}^{2+}]_i$  along the regions indicated by the colored horizontal arrows. For panel *C*, the  $[\text{Ca}^{2+}]_i$  signals in the line-scan images in panels *A* and *B* were masked at a  $[\text{Ca}^{2+}]_i$  value corresponding to 150 nM (solid color lines; mask from panel *A* is the red line and mask from panel *B* is the green line). The velocity of  $[\text{Ca}^{2+}]_i$  signal propagation was calculated from the slope of the derived mask (indicated by the two dashed lines). In the presence of caffeine, the electroporation-evoked  $\text{Ca}^{2+}$  wave had approximately one-third the velocity of the control response.

### Electroporation caused rapid membrane disruption, followed by $\text{Ca}^{2+}$ influx and activation of $\text{Ca}^{2+}$ puffs

With low field intensities, the  $\text{Ca}^{2+}$  influx occurring during the electroporative pulse was small and usually barely detectable, and it was the subsequent regenerative  $\text{Ca}^{2+}$  signals that confirmed electroporation had actually taken place. However, with higher field intensities ( $\geq 750$  V/cm), transient increases in  $[\text{Ca}^{2+}]_i$  were occasionally observed that were far too rapid to be due to regenerative  $\text{Ca}^{2+}$  release from  $\text{InsP}_3\text{Rs}$ . Such  $[\text{Ca}^{2+}]_i$  signals represented the influx of  $\text{Ca}^{2+}$  through the electroporation-induced membrane pores, and thus provided a way of estimating the life-time of these pores. An

example of such a  $\text{Ca}^{2+}$  influx signal is illustrated in Fig. 7. Concomitant with the electroporative pulse, a  $[\text{Ca}^{2+}]_i$  increase was observed at one pole of the cell (Fig. 7*A, B*). The influx signal (Fig. 7*B*) rapidly reached a peak  $[\text{Ca}^{2+}]_i$  of  $\sim 200$  nM, and triggered a more slowly developing regenerative  $[\text{Ca}^{2+}]_i$  increase throughout the cell (Fig. 7*C*). The expanded time course of the influx signal (Fig. 7*D*) and its time derivative (Fig. 7*E*) revealed that the  $[\text{Ca}^{2+}]_i$  increase resulting from membrane disruption lasted for only  $\sim 1$  s, with a rising phase of  $\leq 4$  ms. Such a response can only arise via near-instantaneous  $\text{Ca}^{2+}$  entry after membrane disruption, followed by rapid membrane resealing. We therefore conclude that the lifetime of the electroporation-induced membrane pores is in the range of  $\sim 1$ – $2$  ms.

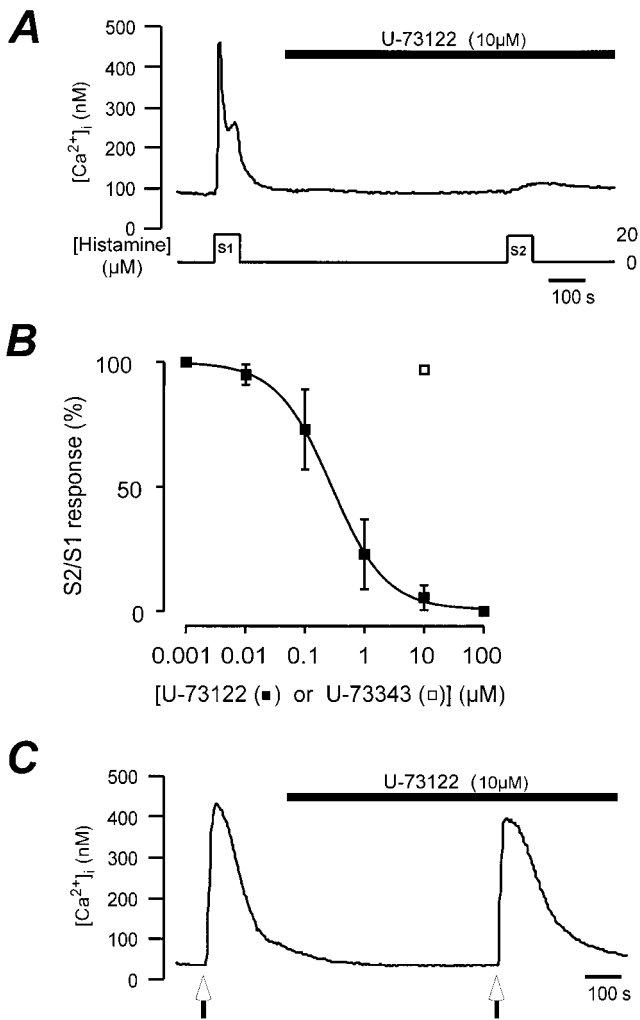


**Figure 6.** Inhibition of hormone- but not electroporation-evoked  $[Ca^{2+}]_i$  signals by U-73122. *A*) An example of inhibition of the histamine-evoked  $[Ca^{2+}]_i$  signal by 10  $\mu M$  concentration of U-73122 (averaged response;  $n=25$ ). *B*) The concentration-dependent inhibition of histamine-evoked  $[Ca^{2+}]_i$  responses in HeLa cells (20  $\mu M$  histamine;  $n=21-37$ ) by U-73122 (filled squares) but not U-73343 (open square). Panel *C* shows the lack of effect of U-73122 (10  $\mu M$ ) on electroporation-evoked  $[Ca^{2+}]_i$  signals (1000 V/cm; 50  $\mu s$  duration; monopolar pulse; averaged response;  $n=27$ ).

To more closely monitor the effect of the electric field on the plasma membrane and its subsequent breakdown, we used the rapid voltage-sensitive indicator di-8-ANEPPS. Upon application of an electroporative pulse, a sudden change in membrane potential occurred in the regions of the cells most closely opposed to the electrodes (**Fig. 8A**). The change in membrane potential correlated with the position of the cell relative to the electrodes; the membranes facing the anode or cathode displayed hyperpolarization or depolarization, respectively (**Fig. 8A**).

Two significant observations can be gleaned from the measurement of the di-8-ANEPPS signals. First, the electroporation-induced voltage change peaked

and then started to decline within 0.5 ms of the start of the pulse (**Fig. 8B**), even though the intensity of the field was constant during the exposure, which lasted for 1 ms (data not shown). The recovery of the membrane potential during the application of the electroporative pulse indicated that the resistance of the membrane rapidly decreased, and consequently that pores had been formed. Second, the change in membrane potential can be repeatedly elicited at a frequency of up to 10 Hz (**Fig. 8C**), indicating rapid recovery of the membrane resistance, i.e., that the membrane has resealed. This showed that electroporation with pulses of 10-fold longer duration than

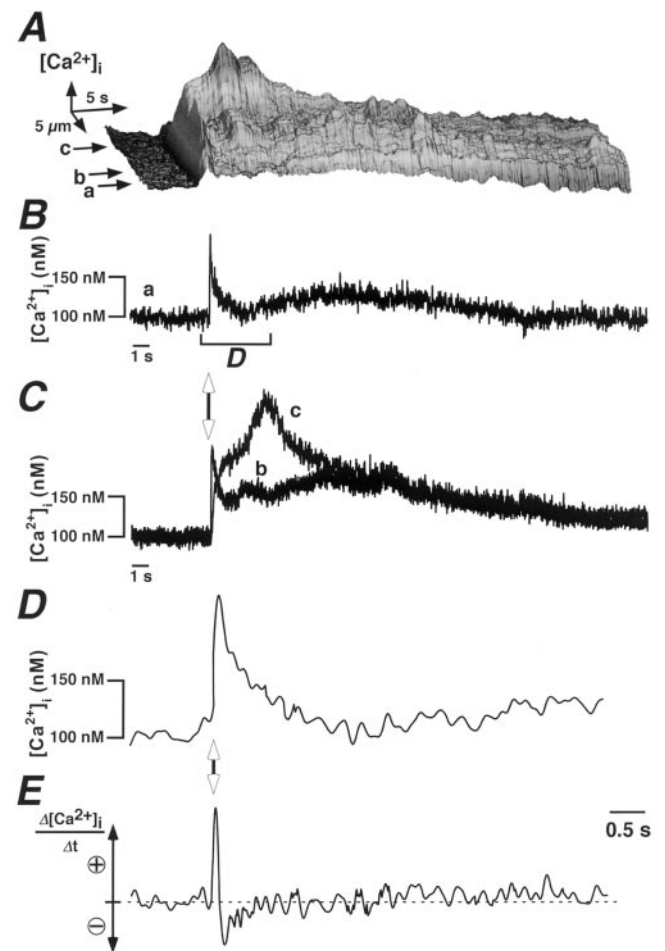


**Figure 7.** Rapid  $[Ca^{2+}]_i$  increase arising directly from  $Ca^{2+}$  influx. *A-E*) Spatial and temporal profile of  $[Ca^{2+}]_i$  in an electroporated HeLa cell (500 V/cm; 100  $\mu s$  duration; bipolar pulse), which displayed a rapid  $Ca^{2+}$  influx signal. Such responses were observed in a minority of cells (<5%;  $n=90$ ). The electroporative pulses were applied at the times indicated by the vertical arrows. *A*) Surface representation of the evoked  $[Ca^{2+}]_i$  rise. The  $[Ca^{2+}]_i$  signals along the regions shown by the horizontal arrows are depicted in panels *B* and *C*. The rapid  $Ca^{2+}$  influx signal is shown in panel *B*, and the subsequent regenerative response is illustrated by the traces in panel *C*. To more clearly illustrate the rapid  $Ca^{2+}$  influx signal in panel *B*, the signal and its derivative are shown on an expanded time scale in panels *D* and *E*, respectively.

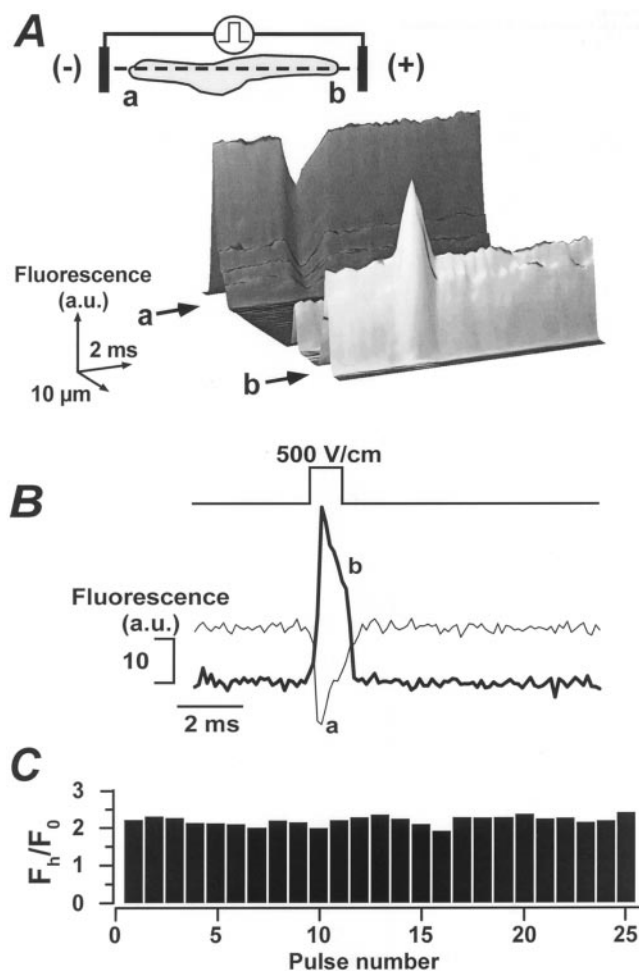


**Figure 8.** Electroporation-induced changes in membrane potential measured with di-8-ANEPPS. *A, B*) The effect of an electroporation pulse (500 V/cm; monopolar pulse; 1 ms duration) on the membrane potential of the single HeLa cell. The surface plot (*A*) and line traces (*B*) show the change of di-8-ANEPPS fluorescence, with downward or upward deflection indicating depolarization (*a*) or hyperpolarization (*b*), respectively. The lines above the figures show the timing of the pulse. The region of the cell chosen for line scanning is shown in panel *A* (dashed line on inset cell image). The bar chart (*C*) shows the ratio between peak fluorescence during the field stimulation at hyperpolarized side of the cell ( $F_h$ ) and resting fluorescence of the same membrane site ( $F_0$ ) for each of 25 consecutive monopolar pulses (500 V/cm, 1 ms, 10 Hz).

those used to evoke  $\text{Ca}^{2+}$  signals in this study did not impose long-term membrane disruptions.

In the majority of cases, where electric fields of modest intensities were used,  $[\text{Ca}^{2+}]_i$  increases arising directly from  $\text{Ca}^{2+}$  entry were difficult to detect. Instead, there was usually a variable latency of up to a few seconds between the electroporative pulse and the onset of a  $[\text{Ca}^{2+}]_i$  signal, suggesting that the rapid undetectable  $\text{Ca}^{2+}$  influx had activated  $\text{Ca}^{2+}$  release (**Fig. 9Aa**). Although the exact nature of the  $[\text{Ca}^{2+}]_i$  signal triggered by electroporation varied with the magnitude of the electroporative pulse, the

most common response to low field intensities ( $\leq 750$  V/cm) was the activation of  $\text{Ca}^{2+}$  puffs.

We earlier determined the nature of hormonally induced  $\text{Ca}^{2+}$  puffs in HeLa cells (4, 13), and found them to be rapid (rise time,  $< 100$  ms) and highly localized (full width at half maximum; FWHM up to 6  $\mu\text{m}$ ). Electroporation evoked similar elementary events, usually occurring in the regions of the plasma membrane most closely adjacent to the electrodes. These electroporation-induced  $\text{Ca}^{2+}$  puffs temporally and spatially resembled those induced by a hormone; they were visualized as spatially confined  $[\text{Ca}^{2+}]_i$  increases, with an FWHM of 2–7  $\mu\text{m}$  (**Fig. 9Ab**). A single  $\text{Ca}^{2+}$  puff was the most common response to an individual electroporative pulse, although trains of  $\text{Ca}^{2+}$  puffs were sometime evoked (**Fig. 9B**).

### The transition between nonregenerative and regenerative responses was dependent on electroporation intensity and frequency

Although the electroporation-induced  $\text{Ca}^{2+}$  puffs originated beneath the regions of the plasma membrane most closely opposed to the electrodes, their exact location was unpredictable. In addition, the threshold field intensity required to evoke  $\text{Ca}^{2+}$  puffs differed both between cells and between various parts of individual cells (data not shown). However, once a threshold stimulus intensity had been found to elicit  $\text{Ca}^{2+}$  puffs, pulsatile application of that voltage triggered repetitive  $[\text{Ca}^{2+}]_i$  transients in the same cellular location. The reproducible induction of  $\text{Ca}^{2+}$  puffs allowed us to investigate the modes of recruitment of such elementary events that induce globally regenerative  $[\text{Ca}^{2+}]_i$  signals.

As illustrated in **Fig. 2A**, the intensity of the electroporation pulse applied to the cells determined the likelihood of triggering a regenerative  $[\text{Ca}^{2+}]_i$  signal. Subthreshold field intensities gave rise to discrete  $\text{Ca}^{2+}$  puffs, which at best triggered only a limited degree of local regeneration (**Fig. 9B** and **Fig. 10**). Despite repeated applications, such low-intensity fields did not trigger global  $[\text{Ca}^{2+}]_i$  signals. However, increasing the voltage applied to the cells could switch the response from spatially restricted  $\text{Ca}^{2+}$  signals to a regenerative  $[\text{Ca}^{2+}]_i$  wave (**Fig. 10**).

In addition to the effects of enhancing field intensity, increases in the frequency of electroporative pulses could also induce regenerative  $[\text{Ca}^{2+}]_i$  signals. The sequence of traces shown in **Fig. 11A–D** illustrates the effects of increasing the frequency of a threshold electroporative pulse. At 0.05 or 0.1 Hz, the electroporative pulses evoked low-amplitude  $[\text{Ca}^{2+}]_i$  signals, which were restricted to only a couple of cellular regions (**Fig. 11A, B**). Although

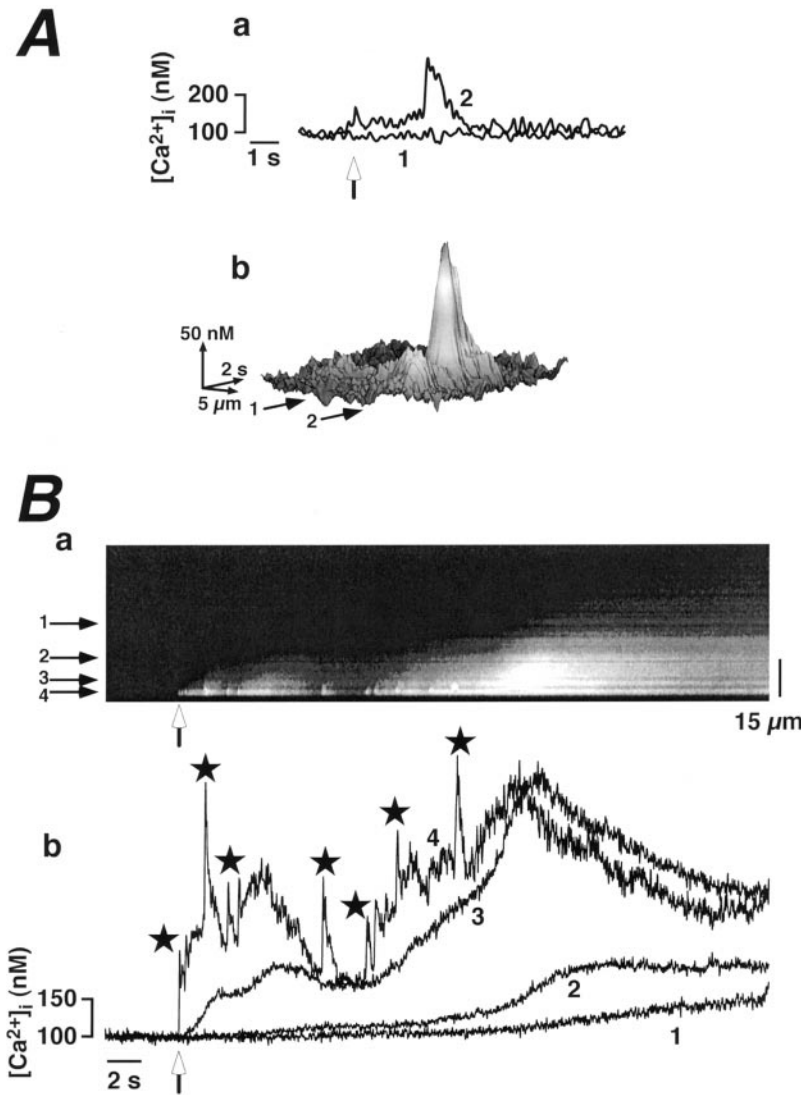


**Figure 9.**  $Ca^{2+}$  puffs and local  $Ca^{2+}$  signals triggered by electroporation. *A, B*) Individual (*A*) and multiple (*B*)  $Ca^{2+}$  puffs evoked by a single electroporative pulse (100  $\mu$ s duration; bipolar pulse). The electroporative pulses were applied at the vertical arrows. For panels *A, B* the field intensities were 400 and 500 V/cm, respectively. *Aa* shows the time course of  $[Ca^{2+}]_i$  in distinct regions of the electroporated cell that gave no response (*Aa1*) or displayed a  $Ca^{2+}$  puff (*Aa2*). To more clearly illustrate the spatio-temporal profile of the electroporation-evoked  $Ca^{2+}$  puff, the event is presented as a surface plot in panel *Ab*. *B*) A train of  $Ca^{2+}$  puffs resulting from a single electroporative pulse. As shown in the line-scan plot in panel *Ba*, these  $Ca^{2+}$  puffs triggered only a limited amount of local regeneration. The  $[Ca^{2+}]_i$  responses along the regions shown by the horizontal arrows are depicted in panel *Bb*. For clarity, the more obvious puffs are marked with an asterisk.

there was some variability, presumably due to changes in the degree of local regenerativity, each electroporative pulse caused a localized  $[Ca^{2+}]_i$

increase. However, even after multiple pulses, a global  $[Ca^{2+}]_i$  signal was not triggered. At 0.2 Hz, spatially restricted  $[Ca^{2+}]_i$  signals were evoked,

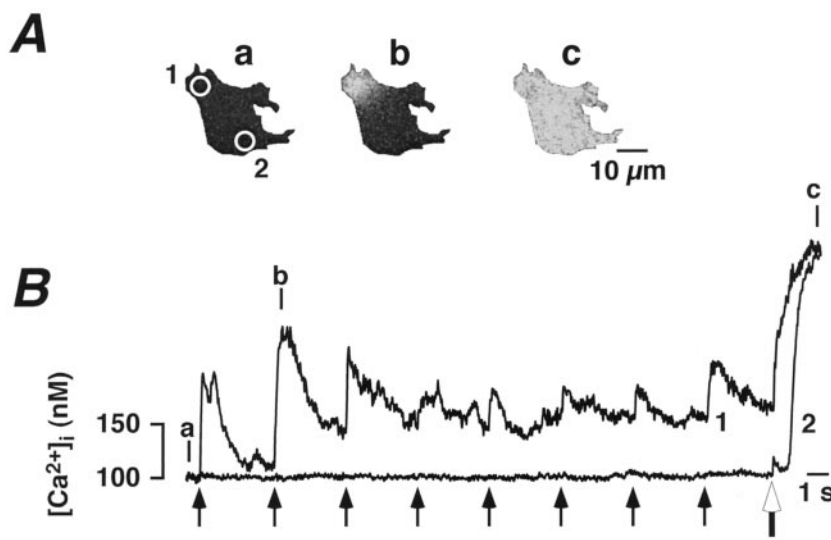


**Figure 10.** Induction of regenerative  $Ca^{2+}$  signals depends on electroporation intensity. Panels *A, B* depict the spatial and temporal profile of  $[Ca^{2+}]_i$  in an individual HeLa cell stimulated repeatedly (0.3 Hz; vertical arrows in panel *B*) with a subthreshold intensity field (400 V/cm; 100  $\mu$ s duration; bipolar pulse), followed by a single (open arrowhead) suprathreshold stimulation (500 V/cm; 100  $\mu$ s duration; bipolar pulse).  $[Ca^{2+}]_i$  in the two cellular regions depicted in *Aa* is plotted in panel *B*. The times at which the cell images in panel *A* were obtained are shown by the vertical lines in panel *B*.

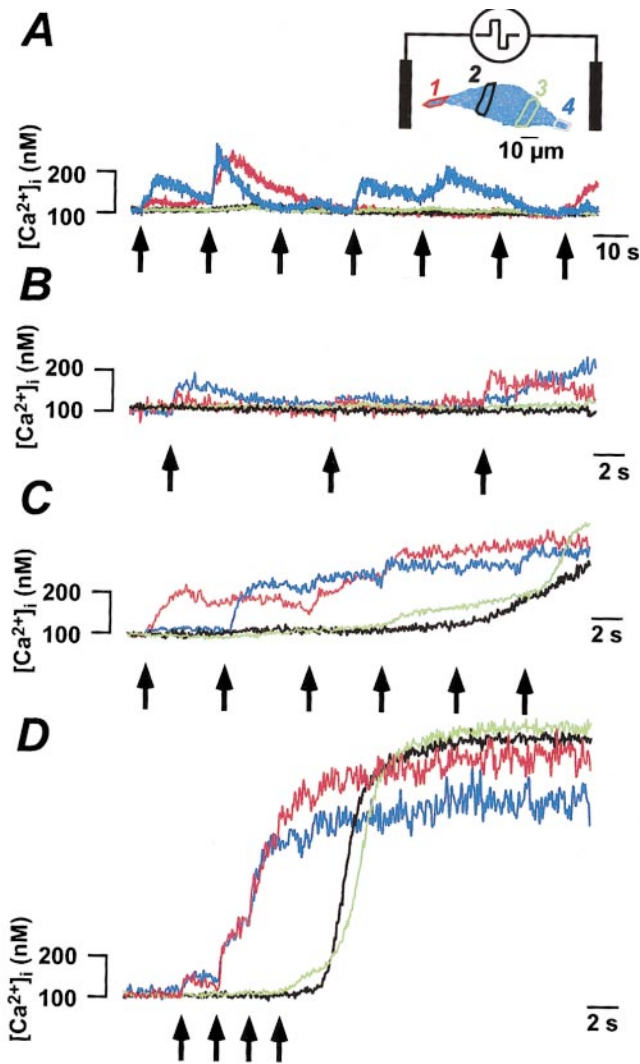


**Figure 11.** Induction of regenerative  $\text{Ca}^{2+}$  signals depends on electroporation frequency. Panels A–D illustrate the response of a single HeLa cell to pulsatile electroporation with a low-intensity (400 V/cm; 100  $\mu\text{s}$  duration; bipolar pulse) at: A, 0.05 Hz; B, 0.1 Hz; C, 0.2 Hz; D, 0.5 Hz. The traces in panels A–D represent the  $[\text{Ca}^{2+}]_i$  response in the four subcellular areas depicted in the cell image, with the time course of the  $[\text{Ca}^{2+}]_i$  signal in each area shown by the corresponding colored line.

which were not able to recover back to basal levels before the onset of the next  $[\text{Ca}^{2+}]_i$  rise. Eventually, the elevated  $[\text{Ca}^{2+}]_i$  in the responsive regions diffused throughout the rest of the cell, causing a uniform  $[\text{Ca}^{2+}]_i$  elevation (Fig. 11C), however, a regenerative  $[\text{Ca}^{2+}]_i$  signal was not triggered. Increasing the frequency of electroporation pulses to 0.5 Hz initially triggered discrete  $\text{Ca}^{2+}$  puffs and eventually led to a regenerative globally propagating  $[\text{Ca}^{2+}]_i$  wave (Fig. 11D).

## DISCUSSION

We have used electroporation to evoke small and brief  $\text{Ca}^{2+}$  influx events into restricted subplasma-

lemmal regions of HeLa cells, and investigated their subsequent ability to trigger local and global responses. The main reason for using electroporation in this way is that it is substantially more reproducible and controllable than hormone stimulation. In addition, the level of permeabilization at particular parts of the cell can be varied in several ways: field intensity, duration, frequency, and direction. Electroporation acts almost instantaneously, is rapidly reversible, and at low field intensities causes minimal membrane disruption (Fig. 8). An important feature of electroporation is that it allows permeabilization of a small, restricted part of the membrane (Fig. 10), providing control over the timing, amount, and the part of the membrane through which the transmembrane  $\text{Ca}^{2+}$  fluxes are generated.

In HeLa cells, electroporation caused a  $\text{Ca}^{2+}_o$ -dependent  $[\text{Ca}^{2+}]_i$  increase (Fig. 1) that was proportional to the intensity of the electric field applied to the cells (Figs. 2 and 10). Although the electroporation-evoked signals required  $\text{Ca}^{2+}_o$ , the  $[\text{Ca}^{2+}]_i$  increase appeared to arise largely through activation of regenerative  $\text{Ca}^{2+}$  release by intracellular  $\text{Ca}^{2+}$  channels, since it was substantially inhibited by caffeine (Fig. 2A and Fig. 5), required functional  $\text{Ca}^{2+}$  stores (Fig. 2C), and could occur some time after the electroporative pulse (Fig. 4 and Fig. 9A). In addition, whereas electroporation invariably caused  $\text{Mn}^{2+}$  quench of fura-2 (Fig. 1C),  $[\text{Ca}^{2+}]_i$  increases were not always recorded (e.g., third electroporation pulse in Fig. 11A). Furthermore, application of high-frequency electroporation pulses desensitized the  $[\text{Ca}^{2+}]_i$  response (Fig. 3). Together, these observations suggest that a small, usually imperceptible  $\text{Ca}^{2+}$  influx activated regenerative  $\text{Ca}^{2+}$  release from internal stores.

Changes in the concentration of ions other than  $\text{Ca}^{2+}$ —e.g.,  $\text{Na}^+$  and  $\text{K}^+$ —probably occurred during the formation of membrane pores by electroporation. Exact quantitation of changes in these ions was not undertaken during our study. However, we think it is reasonable to assume that the largest flux of ions will be  $\text{Ca}^{2+}$ , as it has the largest electrochemical gradient across the cell. Since we are unable to measure the very small flux of  $\text{Ca}^{2+}$  during weak electroporation events, it is unlikely that we could measure changes in  $\text{Na}^+$  or  $\text{K}^+$ . Furthermore, these ions are much more highly diffusible than  $\text{Ca}^{2+}$  in the cytoplasm, and therefore we would expect any changes in  $\text{Na}^+$  or  $\text{K}^+$  to be rapidly reequilibrated.

It was surprising to observe that electroporation on its own could trigger regenerative  $[\text{Ca}^{2+}]_i$  signals, since the activation of  $\text{InsP}_3\text{Rs}$  is believed to require both  $\text{InsP}_3$  and  $\text{Ca}^{2+}$  (29–35). However, the electroporation-evoked  $[\text{Ca}^{2+}]_i$  responses were not sensitive to the PLC inhibitor U-73122 (Fig. 6), suggesting that it did not look to the cells as if they had been

treated with an agonist. It seems that in the absence of hormonal stimulation, the basal intracellular  $\text{InsP}_3$  concentration is sufficient to allow regenerativity from  $\text{InsP}_3\text{Rs}$ , providing a sufficient trigger  $\text{Ca}^{2+}$  is given. The effect of a subthreshold histamine concentration in sensitizing the cells to low-intensity electroporative pulses (Fig. 3) is consistent with the notion that electroporation-induced  $\text{Ca}^{2+}$  influx and modest intracellular  $\text{InsP}_3$  concentrations can elicit a synergistic effect.

Electroporation of HeLa cells with low ( $<700$  V/cm) field intensities frequently generated  $\text{Ca}^{2+}$  puffs with a similar spatial spreading and time course to hormone-evoked elementary events (Fig. 9). The ability to evoke such localized  $\text{Ca}^{2+}$  signals essentially results from the fact that electroporation is an asymmetric process that disrupts the membrane regions most closely opposed to the electrodes, particularly the membrane portion facing the anode. At low field intensities, only a small area of the plasma membrane may be disrupted, giving a highly localized  $\text{Ca}^{2+}$  influx. We suggest that this small  $\text{Ca}^{2+}$  influx triggers  $\text{Ca}^{2+}$  release from adjacent  $\text{InsP}_3\text{R}$ , thus producing the observed  $\text{Ca}^{2+}$  puffs.

It should be noted, however, that although  $\text{Ca}^{2+}$  puffs were commonly observed, not all electroporation-evoked  $\text{Ca}^{2+}$  signals resembled hormonal  $\text{Ca}^{2+}$  puffs. Application of high-intensity voltages ( $>750$  V/cm) sometimes caused subplasmalemmal  $[\text{Ca}^{2+}]_i$  rises that were too fast to be accounted for by regenerative  $\text{Ca}^{2+}$  release (Fig. 5). These rapid signals most likely arose due to  $\text{Ca}^{2+}$  entry through the electroporation-induced membrane pores. The spatial spread of these signals was also distinct from  $\text{Ca}^{2+}$  puffs, with a semicircular diffusion shell immediately beneath the membrane (data not shown).

Hormone-evoked regenerative  $[\text{Ca}^{2+}]_i$  waves in HeLa cells result from the spatio-temporal recruitment of elementary  $\text{Ca}^{2+}$  events (4, 13). In a previous study, we suggested that the transition from localized elementary events to global  $\text{Ca}^{2+}$  waves is determined by a change in the activity of the elementary signals themselves. Increases in frequency and/or amplitude of the  $\text{Ca}^{2+}$  puffs are required to evoke regenerative  $\text{Ca}^{2+}$  signals (13). Elementary  $\text{Ca}^{2+}$  signals that do not advance in frequency or amplitude fail to trigger global signals. Cytoplasmic integration of the  $\text{Ca}^{2+}$  released during each puff is crucial to allow the ambient level of  $\text{Ca}^{2+}$  to reach the threshold for regenerativity to occur. With subthreshold levels of activity, the  $\text{Ca}^{2+}$  signals arising from individual  $\text{Ca}^{2+}$  puffs have a relatively short cytoplasmic lifetime before being buffered or sequestered. With sufficient activity, the  $\text{Ca}^{2+}$  released during each event overwhelms the cellular buffering mechanisms and is integrated by the cytoplasm to cause a progressive  $[\text{Ca}^{2+}]_i$  increase until the thresh-

old for regenerativity is reached. The reproducibility of electroporation-induced  $\text{Ca}^{2+}$  signals allowed us to overcome the stochastic nature of hormone-evoked  $\text{Ca}^{2+}$  puffs and directly test this scheme.

Increasing the frequency at which low-intensity electroporative pulses were applied enhanced their ability to trigger regenerative  $\text{Ca}^{2+}$  waves (Fig. 11). In addition, the effectiveness of single electroporative pulses in evoking  $\text{Ca}^{2+}$  waves was greater with higher voltages (Fig. 2A and Fig. 10). These data suggest that the electroporation-induced  $\text{Ca}^{2+}$  signals functionally mimic hormone-evoked  $\text{Ca}^{2+}$  puffs in generating regenerative  $\text{Ca}^{2+}$  waves when they provide a suitable trigger.

One significant difference between electroporation-induced events and hormonally stimulated elementary  $\text{Ca}^{2+}$  signals is that whereas the former are evoked beneath the plasma membrane in the periphery of the cells (Figs. 9 and 11), the latter most frequently occur adjacent to the nucleus (36). The reason why agonist-stimulated  $\text{Ca}^{2+}$  puffs are observed largely around the nucleus is unclear. However, the consequence is that a majority of  $\text{Ca}^{2+}$  waves are initiated from perinuclear regions. In contrast, electroporation-induced  $\text{Ca}^{2+}$  waves were initiated far from the nucleus (Fig. 5). These data revealed that different parts of the cytoplasm can be functionally equivalent, and that the location of elementary signals determine initiation sites of regenerative responses.

The qualitative effect of triggering regenerative  $\text{Ca}^{2+}$  waves with particular electroporative frequencies or field intensities was observed whether the electroporation triggered  $\text{Ca}^{2+}$  puffs or simply a direct rapid  $\text{Ca}^{2+}$  entry signal (see above). This suggests that the important criterion for causing regenerative  $\text{Ca}^{2+}$  release is not the location or nature of the activating signal, but simply that a triggering  $[\text{Ca}^{2+}]_i$  threshold has to be attained. [F]

The work was supported by Babraham Institute's DEBS Initiative, the BBSRC, and the Royal Society Cooperation Grant Scheme. The authors would also like to acknowledge the generous support of the EMF Biological Research Trust. M.D.B. is a Royal Society University Fellow.

## REFERENCES

1. Berridge, M. J. (1993) Inositol trisphosphate and calcium signalling. *Nature* (London) 361, 315–325
2. Petersen, O. H., Petersen, C. C. H., and Kasai, H. (1994) Calcium and hormone action. *Annu. Rev. Physiol.* 56, 297–319
3. Yao, Y., Choi, J., and Parker, I. (1995) Quantal puffs of intracellular  $\text{Ca}^{2+}$  evoked by inositol trisphosphate in *Xenopus* oocytes. *J. Physiol.* (London) 482, 533–553
4. Bootman, M. D., Niggli, E., Berridge, M. J., and Lipp, P. (1997) Imaging the hierarchical  $\text{Ca}^{2+}$  signalling system in HeLa cells. *J. Physiol.* (London) 499, 307–314
5. Cheng, H., Lederer, W. J., and Cannell, M. B. (1993) Calcium sparks—elementary events underlying excitation-contraction coupling in heart-muscle. *Science* 262, 740–744

6. Lipp, P., and Niggli, E. (1994) Modulation of  $\text{Ca}^{2+}$  release in cultured neonatal rat cardiac myocytes—insight from subcellular release patterns revealed by confocal microscopy. *Circ. Res.* 74, 979–990
7. López-López, J. R., Shacklock, P. S., Balke, C. W., and Wier, W. G. (1995) Local calcium transients triggered by single L-type calcium channel currents in cardiac cells. *Science* 268, 1042–1045
8. Bootman, M. D., and Berridge, M. J. (1995) The elemental principles of calcium signaling. *Cell* 83, 675–678
9. Parker, I., Choi, J., and Yao, Y. (1996) Elementary events of  $\text{InsP}_3$ -induced  $\text{Ca}^{2+}$  liberation in *Xenopus* oocytes—hot-spots, puffs and blips. *Cell Calcium* 20, 105–121
10. Lipp, P., and Niggli, E. (1996) A hierarchical concept of cellular and subcellular  $\text{Ca}^{2+}$  signalling. *Prog. Biophys. Mol. Biol.* 65, 265–296
11. Berridge, M. J. (1997) Elementary and global aspects of calcium signalling. *J. Physiol. (London)* 499, 291–306
12. Parker, I., and Yao, Y. (1992) Regenerative release of calcium from functionally discrete subcellular stores by inositol trisphosphate. *Proc R. Soc. London B* 246, 269–274
13. Bootman, M. D., Berridge, M. J., and Lipp, P. (1997) Cooking with calcium: the recipes for composing global signals from elementary events. *Cell* 91, 367–373
14. Weaver, J. C. (1993) Electroporation: a general phenomenon for manipulating cell and tissues. *J. Cell Biochem.* 51, 426–435
15. Weaver, J. C., and Chizmadzhev, Y. A. (1996) Theory of electroporation: a review. *Bioelectrochem. Bioenerg.* 41, 135–160
16. Tsong, T. Y. (1991) Electroporation of cell membranes. *Biophys. J.* 60, 297–306
17. Kinoshita, K., Jr., Ashikawa, I., Saita, N., Yoshimura, H., Hiro-yashu, I., Nagayama, K., and Ikegami, A. (1988) Electroporation of cell membrane visualized under a pulsed-laser fluorescence microscope. *Biophys. J.* 53, 1015–1019
18. Hibino, M., Itoh, H., and Kinoshita, K., Jr. (1993) Time courses of cell electroporation as revealed by submicrosecond imaging of transmembrane potential. *Biophys. J.* 64, 1789–1800
19. Kotnik, T., Bobanović, F., and Miklavic, D. (1997) Sensitivity of transmembrane voltage induced by applied electric fields—a theoretical analysis. *Bioelectrochem. Bioenerg.* 43, 285–291
20. Bobanović, F. (1998) Electroporation: a method for introduction of non-permeable molecular probes. In: *Fluorescent and Luminescent Probes*, 2nd Ed (Mason, W. T., ed) Academic Press Ltd., London In press
21. Tekle, E., Astumian, R. D., and Chock, P. B. (1994) Selective and asymmetric molecular transport across electroporated cell membranes. *Proc. Natl. Acad. Sci. USA* 91, 11512–11516
22. Sun, F. Z., Hoyland, J., Huang, X., Mason W. T., and Moor R. M. (1992) A comparison of intracellular changes in porcine eggs after fertilization and electroactivation. *Development* 115, 947–956
23. Teruel, M. N., and Meyer, T. (1997) Electroporation-induced formation of individual calcium entry sites in the cell body and processes of adherent cells. *Biophys. J.* 73, 1785–1796
24. Bootman, M. D., Taylor, C. W., and Berridge, M. J. (1992) The thiol reagent, thimerosal, evokes  $\text{Ca}^{2+}$  spikes by sensitizing the inositol 1,4,5-trisphosphate receptor. *J. Biol. Chem.* 25113–25119
25. Grynkiewicz, G., Poenie, M., and Tsien, R. Y. (1985) A new generation of  $\text{Ca}^{2+}$  indicators with greatly improved fluorescence properties. *J. Biol. Chem.* 260, 3440–3450
26. Hüser, J., Lipp, P., and Niggli, E. (1996) Confocal microscopic detection of potential-sensitive dyes used to reveal loss of voltage control during patch-clamp experiments. *Pflugers Arch.* 433, 194–199
27. Giannini, G., Conti, A., Mammarella, S., Scrobogna, M., and Sorrentino, V. (1996) The ryanodine receptor calcium-channel genes are widely and differentially expressed in murine brain and peripheral tissues. *J. Cell Biol.* 128, 893–904
28. Bennett, D. L., Check, T. R., Berridge, M. J., De Smedt, H., Parys, J. B., Missiaen, L., and Bootman, M. D. (1996) Expression and function of ryanodine receptors in non-excitabile cells. *J. Biol. Chem.* 271, 6356–6362
29. Iino, M. (1990) Biphasic  $\text{Ca}^{2+}$  dependence of inositol 1,4,5-trisphosphate-induced calcium release in smooth-muscle cells of the guinea-pig *Taenia caeci*. *J. Gen. Physiol.* 95, 1103–1122
30. Finch, E. A., Turner, T. J., and Goldin, S. M. (1991) Calcium as a coagonist of inositol 1,4,5-trisphosphate-induced calcium release. *Science* 252, 443–446
31. Bezprozvanny, I., Watras, J., and Ehrlich, B. E. (1991) Bell-shaped calcium response curves of  $\text{Ins}(1,4,5)\text{P}_3$ -gated and calcium-gated channels from endoplasmic-reticulum. *Nature (London)* 351, 751–754
32. Iino, M., and Endo, M. (1992) Calcium-dependent immediate feedback-control of inositol 1,4,5-trisphosphate-induced  $\text{Ca}^{2+}$  release. *J. Gen. Physiol.* 360, 76–78
33. Missiaen, L., De Smedt, H., Parys, J. B., and Casteel, R. (1994) Co-activation of inositol trisphosphate-induced  $\text{Ca}^{2+}$  release by cytosolic  $\text{Ca}^{2+}$  is loading dependent. *J. Biol. Chem.* 269, 7238–7242
34. Bootman M. D., Missiaen L., Parys J. B., De Smedt H., and Casteels R. (1995) Control of inositol 1,4,5-trisphosphate-induced  $\text{Ca}^{2+}$  release by cytosolic  $\text{Ca}^{2+}$ . *Biochem J.* 306, 445–451
35. Missiaen, L., De Smedt, H., Parys, J. B., and Casteels, R. (1996) Threshold for inositol 1,4,5-trisphosphate action. *J. Biol. Chem.* 271, 12287–12293
36. Lipp, P., Thomas, D., Berridge, M. J., and Bootman, M. D. (1997) Nucleoplasmic calcium signalling by individual cytoplasmic calcium puffs. *EMBO J.* 16, 7166–7173

*Received for publication June 9, 1998.  
Revised for publication October 19, 1998.*